IV International Conference on Computational Methods for Coupled Problems in Science and Engineering
COUPLED PROBLEMS 2011
M. Papadrakakis, E. Oñate and B. Schrefler (Eds)

EFFECT OF AGGREGATES AND ITZ ON VISCO-DAMAGED RESPONSE OF CONCRETE AT THE MESO SCALE LEVEL

G. XOTTA, V.A. SALOMONI AND C.E. MAJORANA

Department of Structural and Transportation Engineering
Faculty of Engineering, University of Padua
via F. Marzolo 9 – 35131 Padua, Italy
e-mail: xotta@dic.unipd.it, salomoni@dic.unipd.it, majorana@dic.unipd.it

Key words: meso-scale modeling, model B3, damage, spalling.

Abstract. A deep knowledge on the behavior of concrete materials at the mesoscale level requires, as a fundamental aspect, to characterize aggregates and specifically, their thermal properties if fire hazards (e.g. spalling) are accounted for. The assessment of aggregates performance (and, correspondingly, concrete materials made of aggregates, cement paste and ITZ –interfacial transition zone-) is crucial for defining a realistic structural response as well as damage scenarios. Particularly, it is assumed that concrete creep is associated to cement paste only and that creep obeys to the B3 model proposed by Bazant and Baweja since it shows good compatibility with experimental results and it is properly justified theoretically. The fully coupled 3D F.E. code NEWCON3D has been adopted to perform meso-scale analyses of concrete characterized by aggregates of different types and different thermal conductivities. Damage maps allows for defining an appropriate concrete mixture for responding to spalling and for characterizing the coupled behaviour of ITZ as well.

1 INTRODUCTION

The effect of aggregates on the visco-damaged response of concrete at the meso-scale level is here considered; particularly, model B3 [1, 2] and Mazars' law [3, 4] have been chosen and implemented in the FE code NEWCON3D [5] when considering creep and damage, respectively.

As regards the viscous response, many experiments available in literature have shown that in concrete the source of creep is the cement paste, instead aggregates do not creep in the range of stresses encountered in service. It is therefore reasonable to consider concrete as a composite formed by one aging viscoelastic phase (cement paste) and one elastic phase (aggregate) [6]. Hence model B3, generally adopted to characterize the creep features of concrete, can be successfully used even to model cement paste creep alone [7].

Model B3 has been first validated within NEWCON3D to fit experimental tests at the macro-level [8] and subsequently adopted to perform predictive creep and shrinkage analyses at the meso-level, where concrete is considered as a three-phase composite made of cement paste, aggregate and ITZ.

Additionally, the damaged behavior of concrete at the meso-level has been considered both

to understand the influence of ITZ, the weakest region of the composite material, on the overall mechanical behavior and to define an appropriate concrete mixture for responding to spalling.

2 MODEL B3

Model B3, first developed by Bazant and Baweja in 1995 [1, 2], characterizing concrete creep and shrinkage in the design of concrete structures, shows good compatibility with experimental results and it is better theoretically justified if compared to previous models.

The model distinguishes between Basic Creep (time-dependent deformations where no moisture exchanges with the environment occur) and Drying Creep (additional creep strain accounting for drying).

The compliance function of this model at time t, if a unit uniaxial constant stress is applied at time t', takes the following form:

$$J(t,t') = q_1 + C_0(t,t') + C_d(t,t',t_0) \tag{1}$$

where q_1 is the instantaneous strain due to a unit stress, $C_0(t,t')$ is the compliance function for basic creep and $C_d(t,t',t_0)$ the additional compliance function due to drying, t the current age, t' the age at loading and t_0 the age at the start of drying.

Specifically, the total basic creep compliance is:

$$C_0(t,t') = q_2 \cdot Q(t,t') + q_3 \cdot ln\left[1 + (t-t')^n\right] + q_4 \cdot ln\left(\frac{t}{t'}\right) \tag{2}$$

instead the additional creep due to drying is:

$$C_d(t,t',t_0) = q_5 \cdot \left[exp\{-8H(t)\} - exp\{-8H(t')\}\right]^{1/2} \tag{3}$$

where $H(t)$ and $H(t')$ are spatial averages of pore relative humidity.

As regards q_1, q_2, q_3, q_4, q_5 parameters, Z.P. Bazant has provided a series of relations based on a statistical survey data of the Data Base by RILEM.

3 MAZARS' DAMAGE MODEL

The damage model considered in NEWCON3D is the non-local Mazars' damage one. The stress-strain law is expressed as:

$$\boldsymbol{\sigma} = \boldsymbol{\Lambda}_0 (1 - D) \otimes \boldsymbol{\varepsilon}_e \tag{4}$$

where $\boldsymbol{\sigma}$ and $\boldsymbol{\varepsilon}_e$ are stress and strain tensors, D is the damage parameter and $\boldsymbol{\Lambda}_0$ the initial stiffness matrix of the material.

The response of the material takes the following form:

$$f(\boldsymbol{\varepsilon}, \boldsymbol{\Lambda}, K_0) = \tilde{\boldsymbol{\varepsilon}} - K(D) \tag{5}$$

where $\tilde{\boldsymbol{\varepsilon}}$ is the equivalent strain and $K(D)$ the hardening/softening parameter, initially equal to K_0.

Particularly, the response in traction or compression is described by the damage parameters D_t and D_c:

$$D = \alpha_t D_t + \alpha_c D_c, \qquad D_t = F_t(\tilde{\varepsilon}) \quad and \quad D_c = F_c(\tilde{\varepsilon}) \tag{6}$$

$$F_i(\varepsilon_i) = 1 - \frac{(1 - A_i)K_0}{\tilde{\varepsilon}} - \frac{A_i}{exp[B_i(\tilde{\varepsilon} - K_0)]} \qquad (i = t, c) \tag{7}$$

where α_t and α_c are weight coefficients and K_0, A_i and B_i are parameters that can be determined from experimental tests [9].

Considering a non-local approach, the model computes a variable $\bar{\varepsilon}$:

$$\bar{\varepsilon}(\underline{x}) = \frac{1}{V_r(\underline{x})} \int_V \tilde{\varepsilon}(\underline{s}) \alpha(\underline{s} - \underline{x}) dv \tag{8}$$

where $\tilde{\varepsilon}$ is the equivalent strain, $\underline{x}$ the coordinate of the current Gauss point, $\underline{s}$ the coordinate of the generic Gauss point, α the weight function depending on the characteristic length l and V_r is the characteristic volume. For further explanations the reader is referred to [3, 4, 10, 11].

3 CONCRETE AT THE MESO-SCALE LEVEL

Concrete has a highly heterogeneous microstructure and its composite behavior is exceedingly complex. For obtaining a deeper understanding, theoretical studies based on micromechanics analysis of the interaction between various components of concrete have been developed for deducing its macroscopic constitutive behavior. However, microstructure and properties of the individual components of concrete and their effects on the macroscopic overall response have not been deepened enough; such aspects are now analyzed for simulating concrete behavior from the computational viewpoint [12].

As a composite material, concrete is a mixture of cement paste with aggregates inclusions of differents sizes. The components of the heterogeneous material have different properties. The way they react on loading varies too. Variation in stiffness and strength of the components has influence on the global stiffness and fracture behaviour of the material. Different thermal expansion coefficients of the components result in internal stresses (*eigenstresses*) when the global temperature changes. Heat of hydration during hardening and temperature changes during fire are important features as well. Differences in porosity of the components influence the transport and with that also hygral dilation. Different chemical compositions have influence on internal reactions taking place inside the material, which can also be a function of ingress of species [13].

However, concrete is not just a two-phase composite; it has been found that the presence of grains in the paste causes a thin layer of matrix material surrounding each inclusion to be more porous than the bulk of the surrounding cement paste matrix. This layer is called the interfacial transition zone (ITZ), which is known to play an important role in the properties of a concrete composite [14, 15]. The ITZ has a layered structure, a lower density than the bulk matrix and it is more penetrable by fluids and gases [15, 16]; therefore, the ITZ greatly influences the overall permeability of concrete [17]. Additionally, due to its complex structure, the ITZ appears to be the weakest region of the composite material when exposed to external loads. Experiments have demonstrated that the elastic modulus of concrete is strictly related to the elastic modulus and volume fraction of ITZ regions [18, 19]. However, in presence of low w/c ratios and/or fine mineral admixtures (e.g. silica fume), the ITZ may be

absent or difficult to detect. Therefore, the ITZ is not necessarily an intrinsic feature of concrete but depends on factors such as the presence of admixtures, type of mixing, w/c ratio, etc. [20].

As regarding creep features, it is experimentally established that in concrete the only phase subjected to creep is the cement paste; aggregates have essentially an elastic response and cement paste consequently acts as an aging viscoelastic phase. Hence the cement paste is characterized by the aging viscoelastic compliance function $J(t,t')$; particularly, as previously shown, the compliance function adopted here is the one of model B3, being the physical basis of the assumptions used in its derivation also valid for mortar, [6, 7].

4 NUMERICAL ANALYSES.

4.1 Validation of B3 model

To validate B3 model within NEWCON3D, a series of tests by L'Hermite et al. [8] have been taken as reference; specifically, a 7×7×28 cm^3 prism was considered, with the same characteristics as reported in literature (see **Table 1**) and subjected first to basic creep only (specimen kept in water) and subsequently to drying creep (specimen cured in water; at $t_0 = 2$ days exposed to drying).

Table 1: Parameters used for validation of the model (see [21])

Size of the sample [cm^3]	3.5×3.5×14
Elastic Modulus [MPa]	28522.1
f_{cm28} [MPa]	36.3
Cement Content [kg/m^3]	350
Water Content [kg/m^3]	171.5
Aggregate-cement ratio	4.82
Age at the start of dryng t_0 [d]	2
Age of loading t' [d]	7 - 28 – 90
Axial compressive stress [MPa]	9.07
Environmental Relative Humidity	50%
Environmental Temperature [°C]	20

The sample has been additionally loaded by an axial compressive stress of 9.07 MPa; **Figure 1** reports the curves of the compliance function (including drying creep), numerically obtained via the code NEWCON3D once model B3 has been implemented. Three different loading times are considered (7, 28 and 90 days) and a comparison with the curves given by Bazant [21] is depicted, showing a good agreement between numerical and experimentally-based results.

Additionally, the spatial averages of pore relative humidity $H(t)$ and $H(t')$ within drying creep have been replaced with the current relative humidity obtained at each time step from the coupled **u**-H-T system of equations; hence, it has been possible to effectively estimate the humidity variation contribution on the creep term (**Figure 2**).

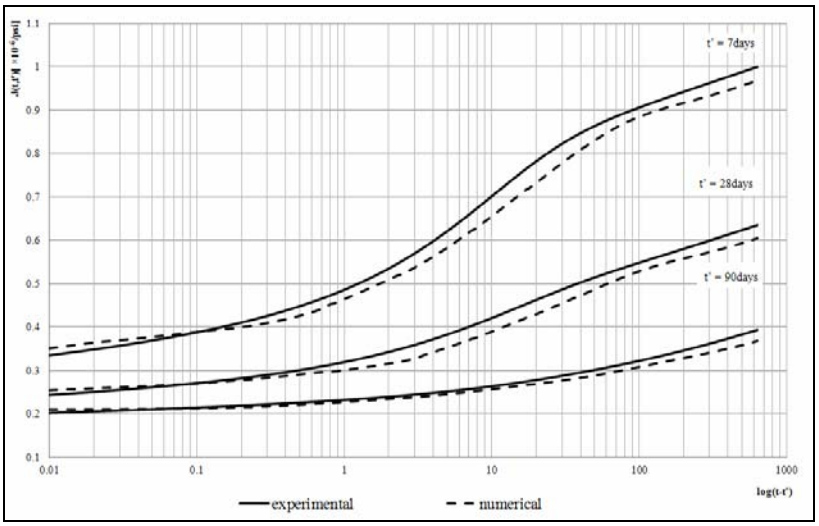

Figure 1: Comparison between compliance curves reported in [8] and obtained via NEWCON3D (dashed lines).

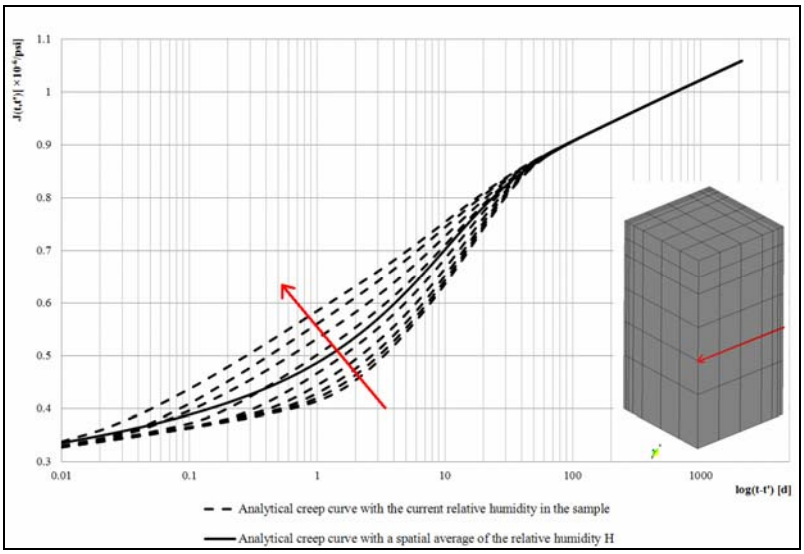

Figure 2: Comparison between analytical creep curves obtained with the spatial average relative humidity (solid line) and with the current relative umidity (dashed lines).

4.2 Numerical Analysis of concrete at the meso-level

If concrete is considered as a composite material made of cement paste and aggregates, the only phases subjected to creep are cement paste and ITZ, whereas aggregates behave elastically, as reported in [6]-[7].

The adopted parameters are listed in **Table 2** and **Table 3**.

The tests by L'Hermite et al. are again taken as reference; the sample is first subjected to basic creep only (specimen kept in water) and subsequently to drying creep (specimen cured in water; at $t_0 = 2$ days exposed to drying at 50% relative humidity and 20°C). The sample is additionally loaded by an axial compressive stress of 9.07 MPa at time t' = 7 days.

Table 2: Meso-scale analysis: parameters for cement paste.

Elastic Modulus [MPa]	28522.1
f_{cm28} [MPa]	36.3
Cement Content [kg/m^3]	350
Water Content [kg/m^3]	171.5
Aggregate-cement ratio	1.5

Table 3: Meso-scale analysis: parameters for aggregates.

Elastic Modulus [MPa]	67000

Figure 3 depicts the evolution of relative humidity within the sample at different times along a section ("A") passing through an aggregate; the physical barrier exerted by the aggregate towards the flux of humidity is clearly evidenced. Consequently, some delay in drying can be noticed when comparing humidity fluxes from the macro-scale analysis (the results are not reported here for sake of brevity).

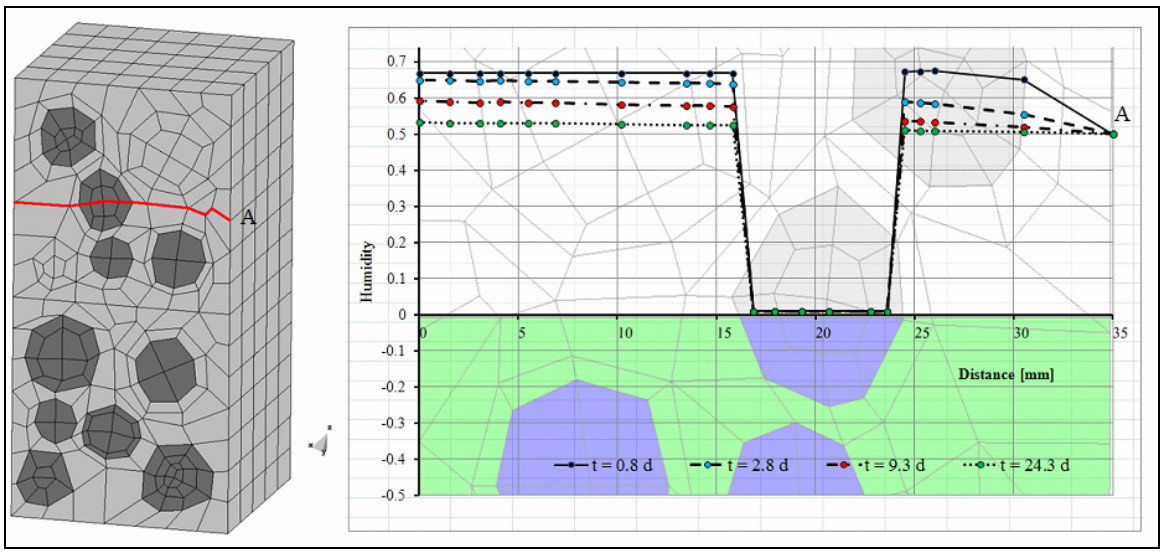

Figure 3: Evolution of relative humidity in the sample at different times for the red line.

A comparison between creep curves for two different points in the cement paste is shown in **Figure 4**: as expected, in proximity of the aggregate, creep effects (hence deformations) are reduced due to a "stiffening effect" coming from the aggregates themselves.

The same concrete sample (3.5×3.5×7 cm^3, in symmetry conditions) has been further considered by including the ITZ and allowing a damage triggering effect; in this way a first estimate of the role of ITZ on the overall mechanical behavior of the concrete sample has been obtained, in view of defining an appropriate concrete mixture for e.g. responding to spalling under high temperature conditions.

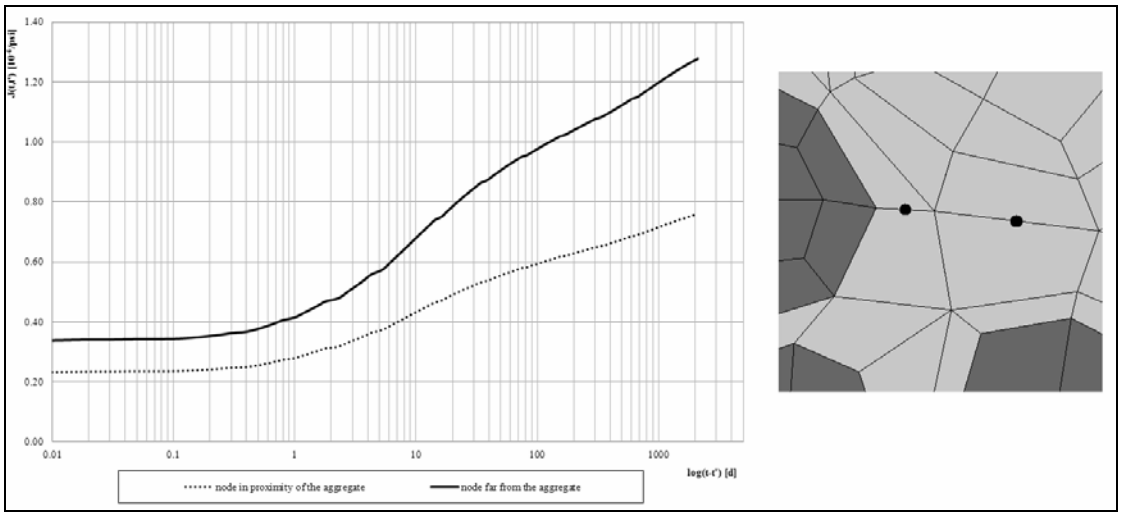

Figure 4: Comparison of the creep function for two nodes of the cement paste.

In **Table 4** and **Table 5** the parameters used for the three different phases as well as for Mazars' damage law are listed.

Table 4: Parameters for cement paste, aggregates and ITZ.

	CEMENT PASTE	ITZ	AGGREGATE
Elastic Modulus [MPa]	28522.1	10000	67000
Poisson's Ratio	0.15	0.2	0.2
Reference Diffusivity along x,y,z [mm^2/d]	150	300	0
Thermal Conductivity along x,y,x [N/d K]	110000	220000	170000

Table 5: Parameters used for the isotropic Mazar's damage model (cement paste and ITZ).

k_0	1×10^{-4}
A_t	1.2
B_t	5000
A_c	1
B_c	1000
B	1

The sample is subjected to a compressive load, in displacements control so to simulate the non linear material response in the softening regime.

The evolution of damage within the sample is shown in **Figure 5** (reference line on the right) at three different times; particularly, it can be noticed that the peaks (maximum damage) occur in the ITZ, the weakest zone of concrete.

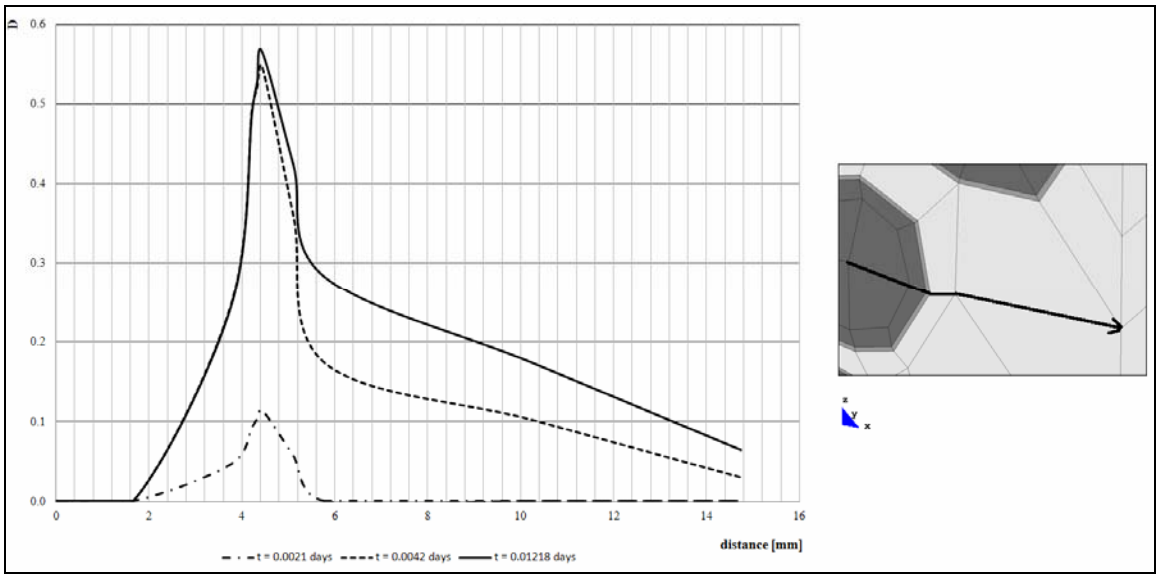

Figure 5: Evolution of damage within the sample at different times for the reference line on the right.

5 CONCLUSIONS

From the previous results some key conclusions can be drawn.

First, the three-dimensionality of the geometric description of concrete at the meso-level can be now appreciated, since 2D or axi-symmetric sections often used in the past were not able to describe with enough precision the complex behaviour of concrete as a composite material. Now this effect can be systematically incorporated due to the availability of powerful computers.

Then, creep of cement paste and ITZ, described by consolidated and complete models as the B3 one presented by Z.P. Bazant (carefully calibrated on the basis of well known experimental results like the ones given by R. L'Hermite), allows to incorporate in the model the complex reality of creep, which is not only a matter of fluid flow and pressure dissipation but also the result of chemical-physical reactions.

Again, the description of concrete as a composite material, in connection with porous media analysis, allows for understanding the hygro-thermal and mechanical response of concrete, first of all in terms of hygral and thermal changes in a material where aggregate inclusions (incapsulated by ITZ concave volumes) appear with some statistical distribution inside concrete (as originally described by F.H.Wittmann, even if without the ITZ effect, [22]).

Hygral barriers due to the presence of aggregates can be seen only at this modelling level. On the other side, thermal conductivity properties dominate the thermal conduction in the sample.

Finally, from the mechanical viewpoint, the remarkable damage peak effect arising from the inclusion of ITZ, if compared with the less pronounced peak when ITZ is disregarded from the analysis, is here reported.

REFERENCES

[1] Bazant, Z.P. and Baweja, S. Creep and shrinkage prediction model for analysis and deign of concrete structures: Model B3. *Adam Neville Symposium: Creep and Shrinkage – Structural Design Effects*, ACI SP – 194 (2000) 1–83.

[2] ACI Committee 209, Guide for Modeling and Calculating Shrinkage and Creep in Hardened Concrete *ACI Report 209*, *2R-08*, Farmington Hills (2008).

[3] Majorana, C.E. Influenza del danno sul comportamento termoigrometrico e meccanico del continuo. *Estratto dal giornale del genio civile*, Luglio, Agosto e Settembre 1989.

[4] Mazars, J., Pijaudier-Cabot, G. and Pulikowski, J. Steel-concrete bond analysis with non local continuous damage. *Rapport Interne No. 96*, March 1989.

[5] Salomoni, V., Majorana, C.E., Mazzucco, G., Xotta, G. and Khoury, G.A. Multiscale modelling of Concrete as a Fully Coupled Porous Medium. *Concrete Materials: Properties, Performance and Applications*, Ch. 3, NOVA Science Publishers (2009) 171-231.

[6] Granger, L. and Bazant, Z. Effect of Composition on Basic Creep of Concrete and Cement Paste. *Journal of engineering mechanics* (1995) **121**.

[7] Baweja, S., Dvorak, G.J. and Bazant, Z.P. Triaxial Composite Model for Basic Creep of Concrete. *Journal of Engineering Mechanics* (1998) 959-965.

[8] L'Hermite, R., Mamillan, M. and Lefèvre, C. Nouveaux résultats de researches sur la déformation et la rupture du béton. *Ann. Inst. Batiment Trav. Publics* (1965) **18**: 323-360.

[9] Mazars, J. Application de la mecanique de l'endommagement au comportament non lineaire et la rupture du beton de structure. *Thèse de Doctorat d' Etat, L.M.T.*, Universitè de Paris, France (1984).

[10] Pijaudier–Cabot, J. Continuum Damage Theory – Application to Concrete. *J Engrg Mech,* ASCE (1989) **115:** 345-365.

[11] Marotti de Sciarra, F. A general theory for nonlocal softening plasticity of integral-type. *International Journal of Plasticity* (2008) **24**: 1411-1439.

[12] Wriggers, P. and Moftah, S.O. Mesoscale Models for concrete: Homogenisation and damage behavior. *Finite El An Des* (2006) **42**: 623-636.

[13] Schlangen, E., Koenders, E.A.B. and Van Breugel, K. Influence of internal dilation on the fracture behavior of multi-phase materials. *Engrg Frac Mech* (2007) **74**: 18-33.

[14] Ollivier, J.P., Maso, J.C. and Bourdette, B. Interfacial Transition Zone in Concrete. *Adv Cem Bas Mat* (1995) **2**:30-38.

[15] Scrivener, K.L., Crumbie, A.K. and Laugesen, P. The Interfacial Transition Zone (ITZ) Between Cement Paste and Aggregate in Concrete. *Interface Science* (2004) **12**: 411-421.

[16] Liao, K.Y., Chang, P.K., Peng, Y.N. and Yang, C.C. A study on characteristics of interfacial transition zone in concrete. *Cem Con Res* (2004) **34**(6): 977-89.

[17] Garboczi, E.J., Bentz, D.P. and Schwartz, L.M. Modeling the Influence of the Interfacial Zone on the DC Electrical Conductivity of Mortar. *Adv. Cement-Based Mater.* (1995) **2**(5): 169–81.

[18] Zheng, J.J. and Zhou, X.Z. A numerical method for predicting the elastic modulus of concrete made with two different aggregates. *J Zhejiang Univ SCIENCE A* (2006) **7**(II): 293-296.

[19] Simeonov, P. and Ahmad, S. Effect of transition zone on the elastic behavior of cement-based composites. *Cem Conc Res* (1995) **25**(1): 165–76.
[20] Garboczi, E.J., Bentz, D.P. and Shane, J.D. Effect of the interfacial zone on the conductivity of Portland cement mortars. *J Am Cer Soc* (2000) **83**(5): 1137-1144.
[21] Bazant, Z. and Kim, J. Improved prediction model for time-dependent deformations of concrete: Part1-7, in *Materials and Structures* (1992) **25**: 21-28.
[22] Wittman, F.H. Surface tension, shrinkage and strength of hardened cement paste. Mat. Struct (1968) **1**(6): 547-552.